Journal of the European Ceramic Society 22 (2002) 2023–2031

www.elsevier.com/locate/jeurceramsoc

R-curve effect, influence of electric field and process zone in $BaTiO_3$ ceramics

Axel Förderreuther, Günter Thurn, André Zimmermann*, Fritz Aldinger

Max-Planck-Institut für Metallforschung and Institut für Nichtmetallische Anorganische Materialien, Universität Stuttgart, Pulvermetallurgisches Laboratorium, Heisenbergstr. 5, 70569 Stuttgart, Germany

Received 15 February 2001; received in revised form 19 November 2001; accepted 2 December 2001

Abstract

Double cantilever beam (DCB) specimens were used to measure fracture toughness and R-curve effect of coarse grained $BaTiO_3$ doped with 0.5 mol% TiO_2 and fine grained $BaTiO_3$ doped with 1.5 mol% La_2O_3 and 3.3 mol% TiO_2. The coarse grained $BaTiO_3$ had an average grain size of 20 μm compared to 0.4 μm for the fine grained material. Coarse grained $BaTiO_3$ showed increasing crack resistance with rising crack length for crack elongations up to 2 mm. The R-curve behaviour can be attributed to mechanisms shielding the crack tip from applied loads, such as ferroelastic domain switching in a process zone ahead of the crack tip, which was observed in situ. Since domain switching events left a pattern on the polished surface of the DCB specimen, it was possible to visualise the domain switching during crack propagation using Nomarski differential interference contrast. The method allowed to measure the size and shape of the process zone in unpoled and poled material. The maximum width of the process zone was 120 μm in both cases but the spatial distribution of switching events showed remarkable differences. An electrical DC field applied to the DCB samples while the cracks were propagating promoted crack growth in coarse grained, unpoled samples. In specimens poled perpendicularly to the crack, a rising toughness was found, if negative electric fields were applied. Fine grained samples were not affected by electrical fields of up to 1 kV/mm.

Keywords: $BaTiO_3$; Domain switching; Grain size; Process zone; R-curve; Toughness

1. Introduction

Ferroelectric toughening has been observed in many investigations of $BaTiO_3$ and PZT ceramics.[1–4] Cook et al.[1] showed that in the ferroelectric state, $BaTiO_3$ has an R-curve effect and a higher fracture toughness than in the paraelectric state. Pohanka et al.[2] observed that the fracture toughness of ferroelectric $BaTiO_3$ increased with increasing grain size, while the fracture toughness for the cubic phase was independent of the grain size.

It is generally believed that domain wall movement under mechanical and electric fields is responsible for the toughening effect.[1,2] The domain wall movement under the influence of an electric field was observed in situ by Oh et al.[5] who investigated thin sections of $BaTiO_3$ with polarised light. When applying an electric field to the specimens, a 90° switching of the domains was reported. The domains did not switch back, unless an electric field in the opposite direction was applied. Arlt[6] described the domain pattern as a result of the minimisation of the strain energy and the domain wall energy. It was shown that the domain distribution in thin sections with a thickness smaller than the grain size, is different from the domain structure of a grain inside a three-dimensional body. Therefore the domain wall movement in thin sections, which is easily observable using polarized light[5] does not correspond to the conditions in bulk specimens. Alternatively, the domain structure of barium titanate bulk ceramics was investigated using voltage-modulated atomic force microscopy.[7] This method has a very high resolution compared with others like the etching of the surface of a specimen or the application of polarised light on thin sections. However, it is almost impossible to observe domain switching in situ with this method.

The proposed mechanism for ferroelastic toughening[8,9] is similar to the well known transformation toughening observed for ZrO_2. Domain switching in

* Corresponding author.
E-mail address: zimmermann@mf.mpg.de (A. Zimmermann).

0955-2219/02/$ - see front matter
PII: S0955-2219(01)00516-7

front of the crack tip is assumed to be induced by mechanical stresses. The transformed zone with altered domain configuration ahead of the crack is later on found in the wake, when the crack tip moves during further crack growth. The strain caused by domain switching leads to compressive stresses which close the crack and lead to an increase of fracture toughness. The effectiveness of ferroelastic toughening depends on the distribution of domain orientation, while stress-induced phase transition in ZrO_2 is coupled with a volume expansion and, thus, independent of orientation effects.[10]

The orientation dependence of ferroelastic toughening was mostly studied with poled or unpoled samples under the simultaneous action of mechanical and electric fields.[3,8,11–14] Since there are many possible configurations for the respective orientation of crack, poling direction and applied field, the results are not always easy to compare and have found various conflicting interpretations. However, stress-induced domain switching provides a likely explanation for many of the experimental observations.

One study should be emphasised which focuses on the orientation dependence of the toughening effect under purely mechanical load.[15] This study clearly reveals that the plateau toughness is higher for unpoled samples than for specimens with poling direction perpendicular to the crack, since the domain orientation is already favourable for the considered poling direction. If the poling direction is chosen parallel to the crack plane, the plateau toughness depends on the specimen dimensions. It was found that increasing specimen dimensions lead to mechanical clamping, which hinders domain switching and, thus, ferroelastic toughening.

It is the objective of the current work to present a new method to visualise the process zone in ferroelectric bulk ceramics during crack propagation in situ and to correlate these results with experimental data on the fracture toughness and the R-curve behaviour for various poling states and microstructures.

2. Experimental

2.1. Sample preparation

Johnson Mattey powder Nr. 88267 (99.9% $BaTiO_3$, mean diameter $\leqslant 2$ μm) was used for the preparation of specimens. Coarse grained barium titanate was prepared using 0.5 mol% TiO_2 as the sintering additive. To suppress grain growth, $BaTiO_3$ was doped with 1.5 mol% La_2O_3 and 3.3 mol% TiO_2. The powders were cold isostatically pressed at a pressure of 625 MPa and sintered for 2 h in a flowing oxygen atmosphere at a temperature of 1350–1450 °C. The coarse grained material showed an Archimedes density of 5.91 g/cm^3, and the average grain size was determined to be 20 μm.

In triple points a secondary phase consisting mainly of $Ba_6Ti_{17}O_{40}$ and impurities of the powder was observed. Quantitative image analysis revealed a porosity between 1 and 3% as well as 0.8 and 1.8% secondary phases. The fine grained $BaTiO_3$ showed a density of 5.78 g/cm^3 and an average grain size of 0.4 μm. Respective microstructures for the coarse and fine grained material are provided in Fig. 1.

Some of the specimens were poled in a silicon oil bath (Wacker TR50). For the poling, a 20 nm chrome layer and subsequently a 200 nm gold layer were sputtered as electrodes on the lateral surfaces of the specimens. The chrome layer acts as a diffusion barrier. The specimens were placed in the oil bath at room temperature. The oil was then heated to 130 °C, and a field of 1.5 kV/mm was applied to the specimens. The heating of the oil bath was switched off, and the specimens were cooled down to room temperature under applied voltage.

2.2. Measurement of the R-curve effect

The R-curve effect was measured using double cantilever beam (DCB) specimens loaded under constant displacement. This choice implements two advantages.

1. The height of the specimen is much smaller than in case of CT-specimens. Thus, an electric field

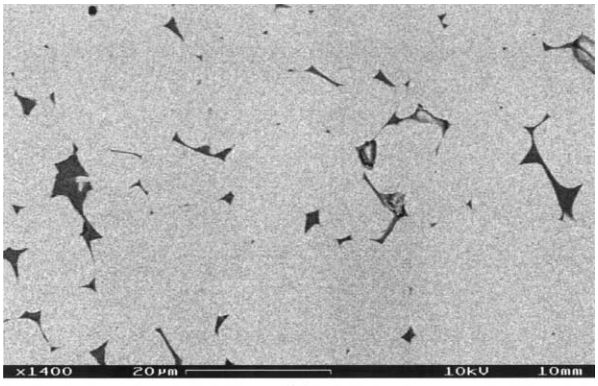

(a)

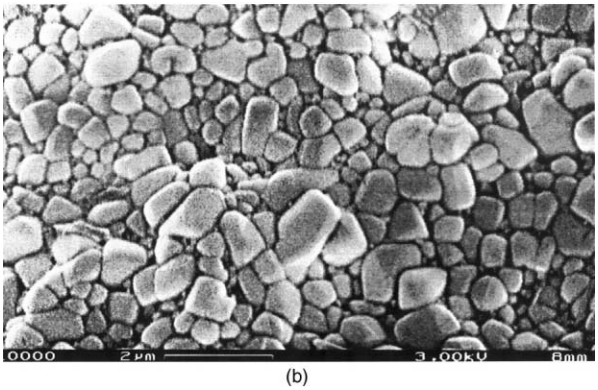

(b)

Fig. 1. Micrographs of coarse grained (a) and fine grained (b) $BaTiO_3$.

perpendicular to the crack can easily be applied in air, since the required voltage is moderate.
2. Loading under constant displacement conditions leads to stable crack growth which can easily be observed in situ.

The specimen size was $16\times4\times4$ mm^3. All surfaces were ground and polished. A notch with a depth of 2.3 mm was introduced into the middle of one of the square sides of the specimens. The notch was ground manually with a razor blade and 3 μm diamond paste. A groove was cut at the backside of the specimens along the axis of the specimens to guide the cracks during crack propagation. The crack propagation was initiated by a ZrO_2 wedge which was introduced into the notch of the specimen (Fig. 2). The crack mouth opening displacement (CMOD) was measured optically.

The crack propagation was observed with an optical long-distance microscope which was mounted on a stage with a two-axis displacement measuring system.

The microscope was equipped with a CCD camera which was connected to a digital video recorder and a monitor. The crack length was determined from the position of the crack tip on the screen and the crack mouth opening displacement with an optical extensometer. The wedge was driven by an actuator with a maximum displacement of 80 μm. The crack propagation was stable, and the velocity of the crack was controlled by the displacement rate of the actuator. During some experiments, an electrical DC field was applied perpendicular to the crack. The experiments with and without electric field have been carried out in air. From the crack length c, the CMOD δ_l, the height h of the specimen and the elastic properties, e.g. Young's modulus E and Poisson's ratio ν, the fracture toughness can be calculated using an expression[16] which is based on the analytical solution of Kanninen.[17]

$$K_{Ic} = \frac{\delta_l \sqrt{3} E/(1-\nu^2)}{2\sqrt{h}\left(\frac{c}{h}+0.64\right)^2} \quad (1)$$

For constant displacement conditions, the stress intensity factor [Eq. (1)] is independent of the specimen thickness.[17]

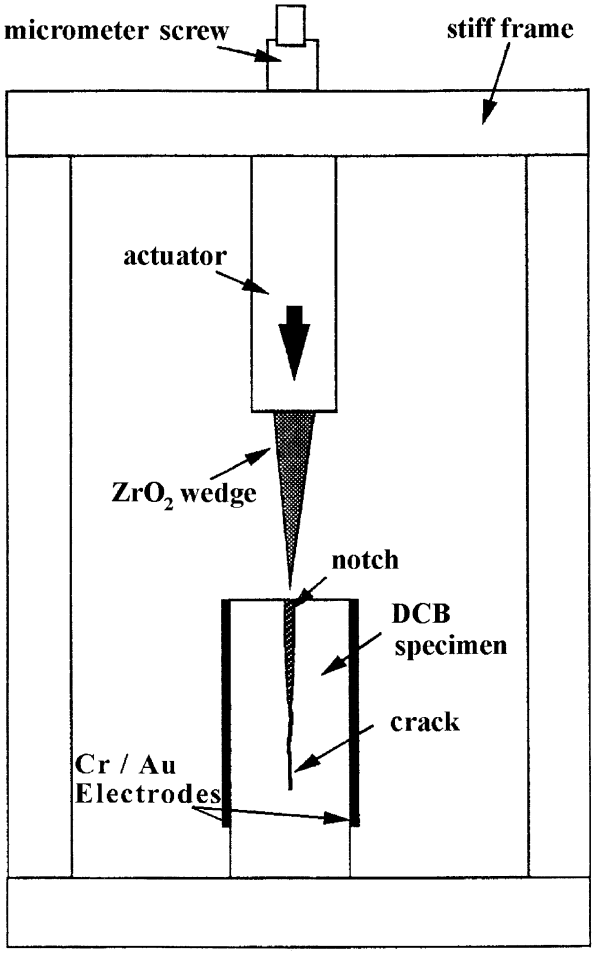

Fig. 2. DCB setup for K_{Ic} measurements. The electrical field is oriented perpendicular to the crack.

2.3. Investigation of the process zone

The same DCB specimens which were used for the measurement of the R-curves were utilised for the investigation of the process zone during crack propagation. Since the investigation of the process zone requires Nomarski contrast the testing equipment had to fit in a conventional optical microscope. It, therefore, consisted of a slim brass frame which held the micrometer screw driving the wedge. The crack was driven manually using the screw which in turn moved the wedge into the notch. During crack propagation the crack tip was observed with an optical microscope (Leitz DM-RME) using Nomarski differential interference contrast with a magnification of 200×. To improve the contrast, a 10 nm gold layer was sputtered onto the surface.

A digital video recorder with 25 frames per second was used to record the crack propagation. The reorientation of a number of domains in the process zone leads to a surface relief due to the related deformation which yields a visible contrast using the Nomarski interference effect. In order to count the domain switching events, the neighbouring images separated by a time interval of 0.04 s were compared with each other. A grid with 39×39 elements was superimposed on the images with the origin located at the crack tip. Each element of the grid covers an area of 5×5 μm^2. If a visible difference within one element of the grid could be detected by comparison of two subsequent images, this was considered as one count. Thus, a count does not represent an individual domain switching event, but a certain number of events occurring in an area with defined position relative to the

crack tip. The mere comparison of one pair of images leads to a spatial distribution of switching events which is statistically insignificant. Thus, the shape of the process zone was evaluated by accumulating the counts from many pairs of neighbouring images recorded during the crack growth. During crack propagation, the grid was moved with the crack tip, such that the crack tip was always kept at the origin. Accordingly, all switching events refer to the actual position of the crack tip in order to accumulate statistically relevant information, although areas which undergo domain switching are certainly found in the wake after crack propagation.

3. Results

3.1. Crack resistance and R-curve effect

Fig. 3 shows the R-curves of seven unpoled $BaTiO_3$ specimens. The crack resistance of the coarse grained samples increases with crack length. The starting value of the R-curves is between 1.3 and 1.4 MPa$\sqrt{}$m. In most cases, a plateau value in the order of 2.2 MPa$\sqrt{}$m was found after a crack elongation of 2 mm, while the plateau was probably not yet reached for sample 4B after crack extension of 4 mm. The crack resistance of fine grained $BaTiO_3$ showed no R-curve behaviour at all, and the fracture toughness was found to be 1.05 MPa$\sqrt{}$m. The crack resistance of the fine grained, unpoled samples 2–4 and 2–5 remained unaffected by an electric field perpendicular to the crack plane.

Fig. 4 shows micrographs of typical crack paths found after DCB experiments. In both microstructures, intergranular as well as transgranular crack growth occurred. In coarse grained $BaTiO_3$ however (a), a myriad of side cracks (sometimes running backwards) together with crack deflection, switching events and crack bridging lead to very rough crack flanks. In fine grained $BaTiO_3$, a straight crack path was observed (b).

Since the crack resistance of the fine grained samples remains unaffected by an electric field, further results focus on the coarse grained material. Fig. 5 displays the R-curve of an unpoled coarse grained sample. As in Fig. 3, a rise of the fracture toughness is observed during crack growth, as long as no electric field is applied. Immediately after a field of 750 V/mm perpendicular to the crack is switched on, the toughness starts to drop.

Fig. 6 compares the R-curve of two DCB experiments with coarse grained, poled samples. In both cases, the poling direction is oriented perpendicular to the crack. For specimen 3D, the applied electric field is chosen to be parallel to the poling direction. By comparison with Fig. 3, it remains unclear whether the application of + 750 V/mm affects the crack growth, since tests without electric field yield a very similar R-curve. However, if the applied electric field is antiparallel to the poling direction as in case of sample 7–2 with −625 V/mm, a pronounced rise of

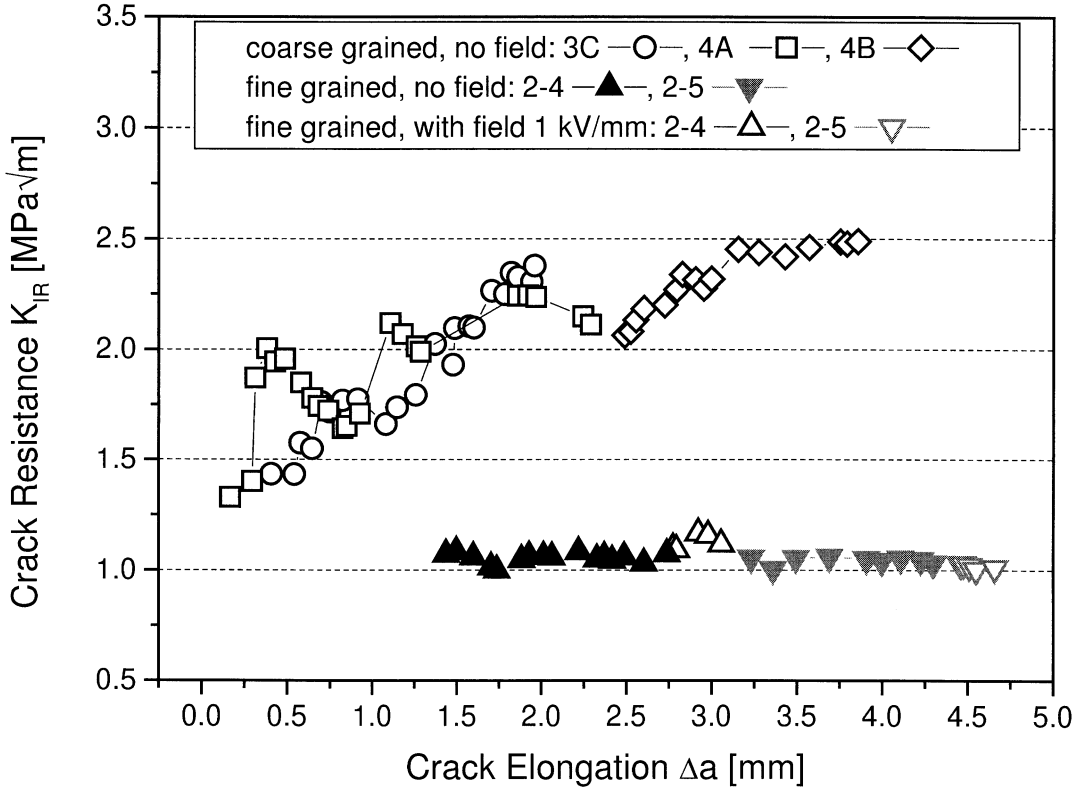

Fig. 3. Comparison of DCB results showing the influence of microstructure on the toughness of $BaTiO_3$.

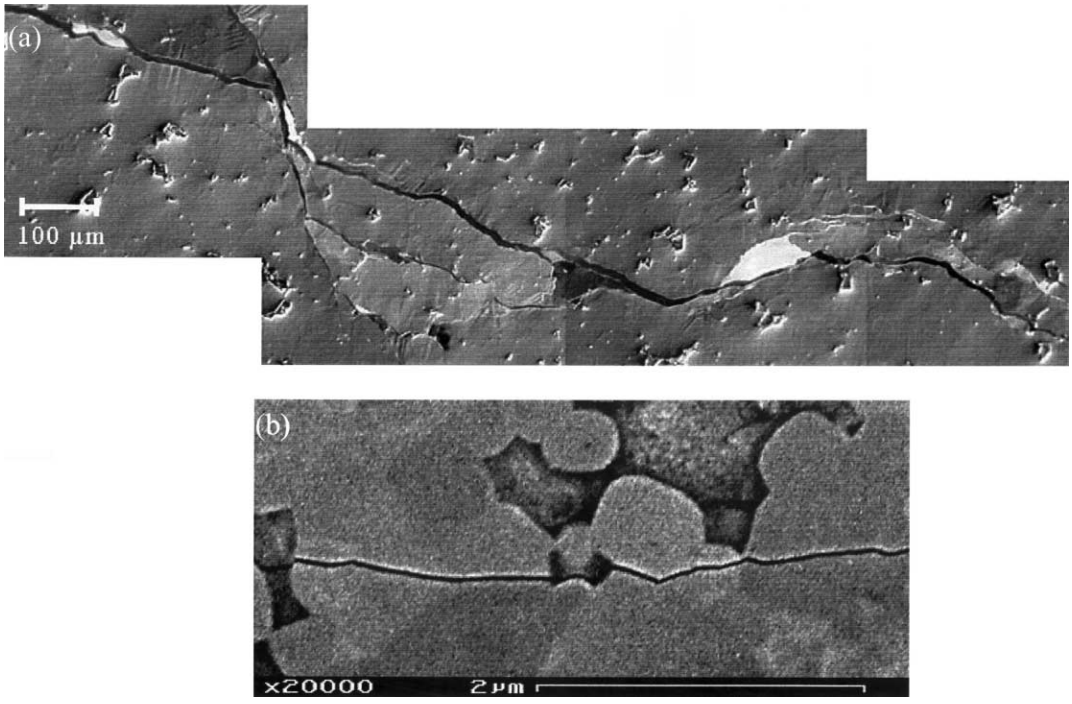

Fig. 4. Optical and SEM micrographs of typical crack paths in coarse grained (a) and fine grained (b) $BaTiO_3$.

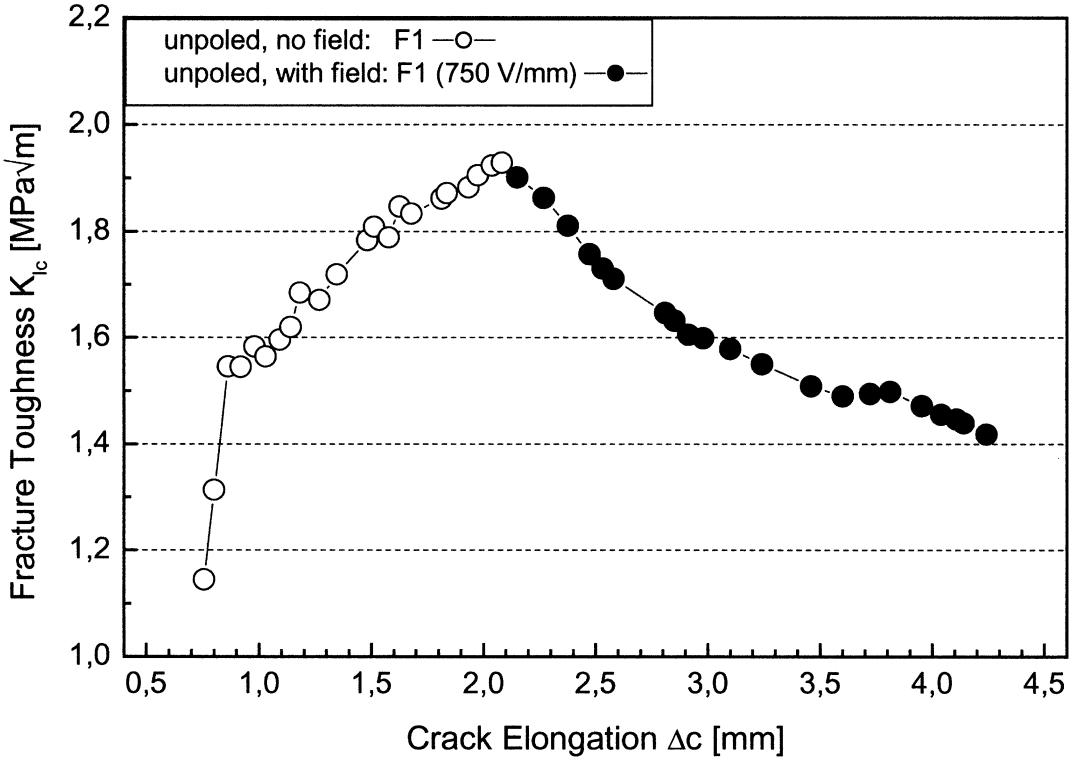

Fig. 5. Influence of DC fields on the toughness of coarse grained, unpoled DCB samples.

toughness is evident, after the field is switched on. When the field is turned off, a time-dependent decrease of toughness can be noted. Measurements of the strain due to domain switching under electric field showed for bulk samples without cracks, that the relaxation of the strain took about 7 s after removal of the electric field. Therefore, this time interval is indicated in Fig. 6. It should be noted that the crack velocity was lower under electric field.

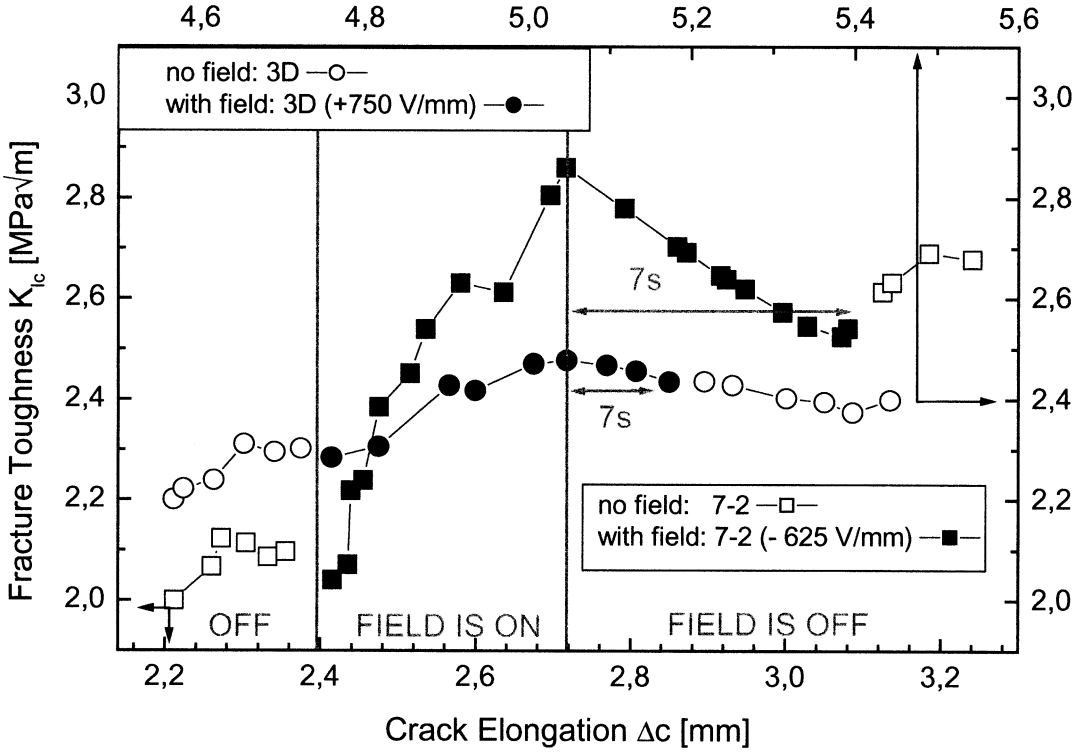

Fig. 6. Influence of DC fields on the toughness of coarse grained DCB samples poled perpendicularly to the crack.

3.2. Process zone

Fig. 7 shows two micrographs from the surface of an unpoled DCB specimen and the change of the surface relief during crack propagation. The crack tip is indicated by an arrow, and the circle around the crack tip has a radius of 150 μm, defining the area in which the domain switching takes place. If the orientation of a number of domains changes, a surface relief develops due to the local deformation caused by domain switching. Many such changes in the height profile of the surface are visible in Fig. 9, e.g. below the crack tip in the lower image.

The influence of poling on shape and size of the process zone is depicted in Figs. 8 and 9. Fig. 8(a) represents the process zone in an unpoled material. During crack propagation of 3.7 mm, 1696 counts of domain switching events were registered equivalent to a density of 458 counts/mm. The highest density of switching events was measured at the crack tip, where 45 counts were registered in a 5×5 μm^2 area. Switching events were observed up to a distance of 120 μm from the crack tip. The maximum distance of switching events was observed under an angle of 45° with respect to the crack. A few switching events were found behind the crack tip.

Fig. 8(b) shows the process zone of a poled specimen. The poling direction is indicated by an arrow, and the orientation was perpendicular to the crack. The amount of switching events was smaller than in the unpoled material. During crack propagation of 5.5 mm only 1230 counts were recorded, yielding a density of 224 counts/mm. The resulting spatial distribution was steeper in the case of the poled material. Some switching events could be detected at a distance of up to 110 μm from the crack tip, which was in the same order as for unpoled materials (120 μm).

Fig. 9 provides two normalised representations of the same distributions as in Fig. 8. In both cases, the core zone, where 50% of the recorded switching events take place, had the shape of an ellipse, with the long axis being oriented perpendicularly to the crack. In the case of unpoled $BaTiO_3$, the ellipse had a length of 50 μm and a width of 30 μm. Poling led to a steeper distribution, such that the size of the elliptical 50% core zone was reduced to 40×16 μm^2.

4. Discussion

The fine grained $BaTiO_3$ samples exhibit no R-curve effect (Fig. 3). Its average grain size of 0.4 μm is well below the critical grain size for the formation of tetragonal domains calculated by Arlt.[5] The grains are, thus, considered to consist mostly of single domains that cannot switch as easily as in coarse grained $BaTiO_3$. Therefore a process zone can not be developed and the material behaves linear-elastic. Furthermore the crack morphology [Fig. 4(b)] shows a total absence of crack tip shielding mechanisms which are prominent in coarse grained $BaTiO_3$.

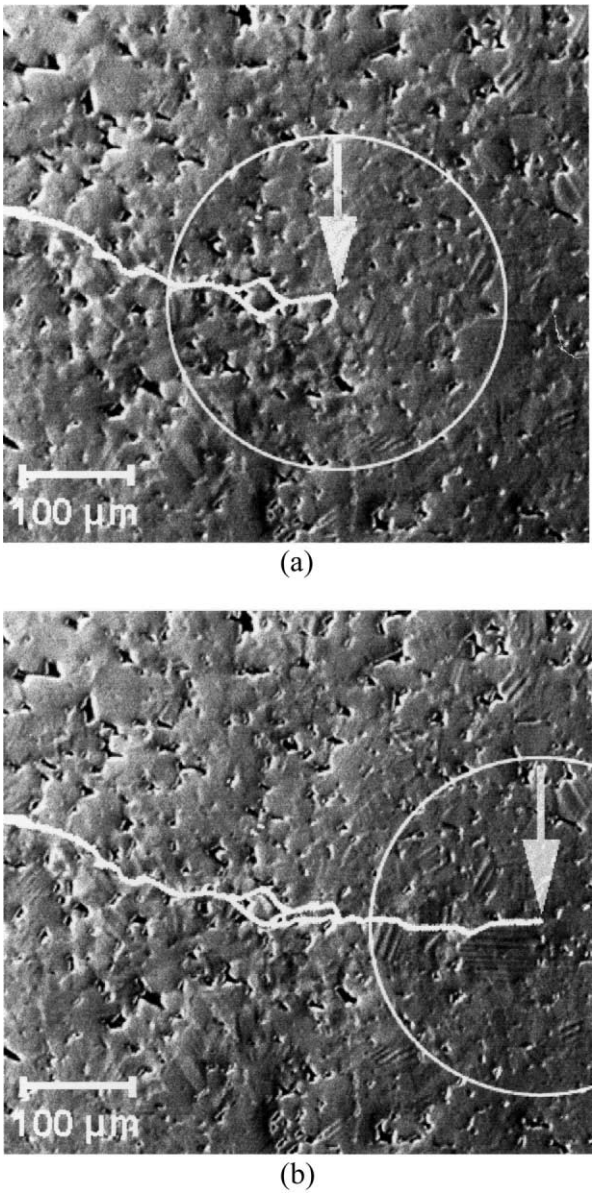

Fig. 7. Micrographs using the Nomarski contrast in order to show a propagating crack in coarse grained $BaTiO_3$ causing domain switching.

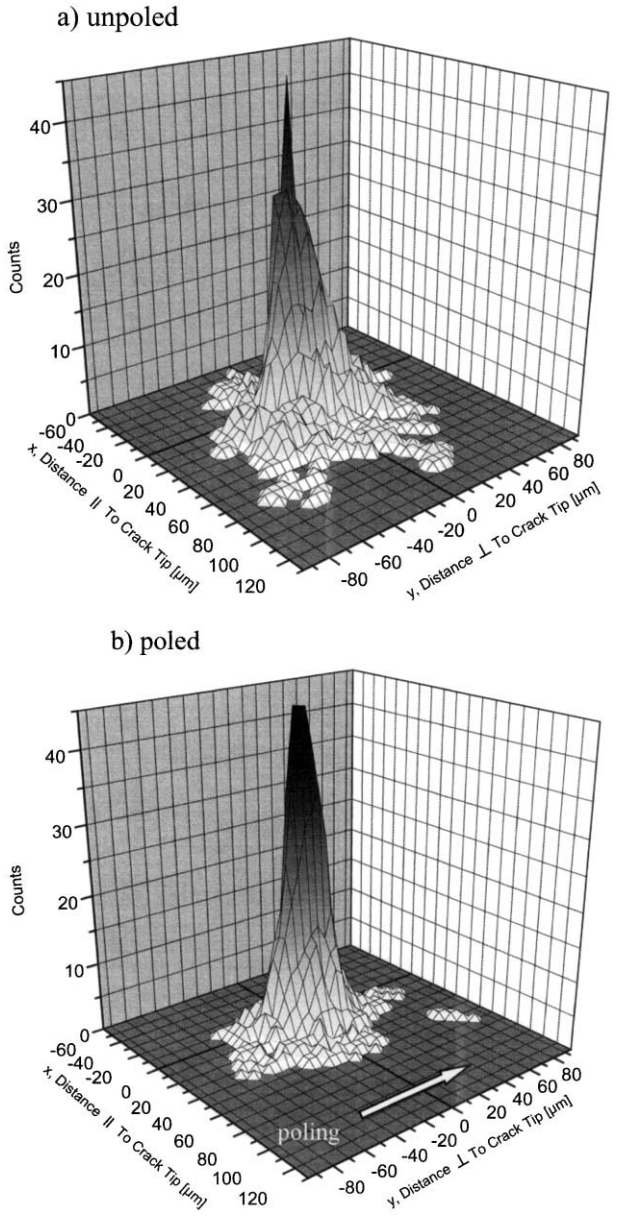

Fig. 8. Distribution of counted domain switching events in (a) unpoled and (b) poled coarse grained $BaTiO_3$. The crack tip is at (0,0), the crack heads towards positive x-values.

For the coarse grained material, the crack path depicted in Fig. 4(a) in conjunction with the observed influence of electric fields on fracture toughness (Figs. 5 and 6) suggest that both crack bridging and ferroelastic toughening contribute to the R-curve effect. The current study focuses on the contribution of ferroelastic toughening which can be derived from the experiments under electric field. The results presented in Figs. 5 and 6 can be explained by stress-induced domain switching ahead of the crack tip. Without electric field, domain switching in unpoled samples is confined to the near-tip region of the crack under high mechanical stresses. The application of an electric field perpendicular to the crack leads to domain switching throughout the entire sample which renders the ferroelastic toughening mechanism at least partially ineffective as seen in earlier work.[15] In accordance with this argument, the toughness of unpoled $BaTiO_3$ is found to decrease after an electric field perpendicular to the crack is switched on (Fig. 5). It can be understood as well that the toughness is not much affected by the electric field, if both the poling direction and the electric field are oriented perpendicularly to the crack. Since most domains throughout the sample are already favourably oriented, ferroelastic toughening is ineffective whether an electric field is applied or not (circles in Fig. 6). If a negative electric field antiparallel to the poling direction is applied, a part of the domains throughout the sample will switch out of the poling

direction. Contrarily, the domains close to the crack tip are preferentially oriented normal to the crack in poling direction due to the applied mechanical stress. As a consequence, the toughness of a sample with poling direction perpendicular to the crack increases, if an electric field antiparallel to the poling direction is applied (squares in Fig. 6). This finding is consistent with previous observations.[8]

In fine grained $BaTiO_3$, shielding mechanisms appear to be absent, hence there is no contribution of crack bridging effects to the fracture toughness. Therefore, a quantification of the ferroelastic toughening effect may be achieved if the fracture toughness of the fine grained $BaTiO_3$ is compared with the starting value of the R-curve for the coarse grained $BaTiO_3$. The difference between the two values amounts to 0.4 MPam. This estimation for the effect of the process zone is in accordance with Ref. [6].

In the following, the shape of the process zone is discussed. Fig. 9 shows that the majority of switching events takes place in a small area around the crack tip, individual events are also observed at a distance of more than 100 μm. It is assumed that intrinsic stresses vary from grain to grain and also within a grain. The exterior stresses from the crack propagation are superimposed to this random stress distribution in the material. Grains where the intrinsic state of stress and the exterior stresses are oriented in the same direction switch more easily than grains where the intrinsic stresses are oriented in the opposite direction. It can be assumed that switching events which occur far away from the crack tip would also take place under a homogeneous stress state. Since the number of switching events in the far field is small, their contribution to the process zone is negligible. Therefore, the characteristic size of the process zone is not the maximum distance of occasional switching events, but the volume in which the majority of switching events occurs. Thus, Fig. 9 describes the core zone where half of the switching events are concentrated. It is evident that the size of this core zone is larger for unpoled samples than for specimens which are poled perpendicularly to the crack. For this poling direction, most of the domains are already found in a favourable orientation, such that higher mechanical stresses are required to cause additional domain switching ahead of the crack tip than for unpoled samples. Since the mechanical stresses decrease rapidly with increasing distance from the crack tip, the core of the process zone is smaller for the poled samples. Beside the geometry of the process zone, the amount of domain switching is an important characteristic. For samples with poling direction perpendicular to the crack, the density of switching events is found to be lower by 50% compared to unpoled samples. Again, this can be explained by the fact that the orientation of domains in the poled samples is preferentially perpendicular to the crack, such that the probability for domain switching under mechanical stresses decreases compared to the unpoled state.

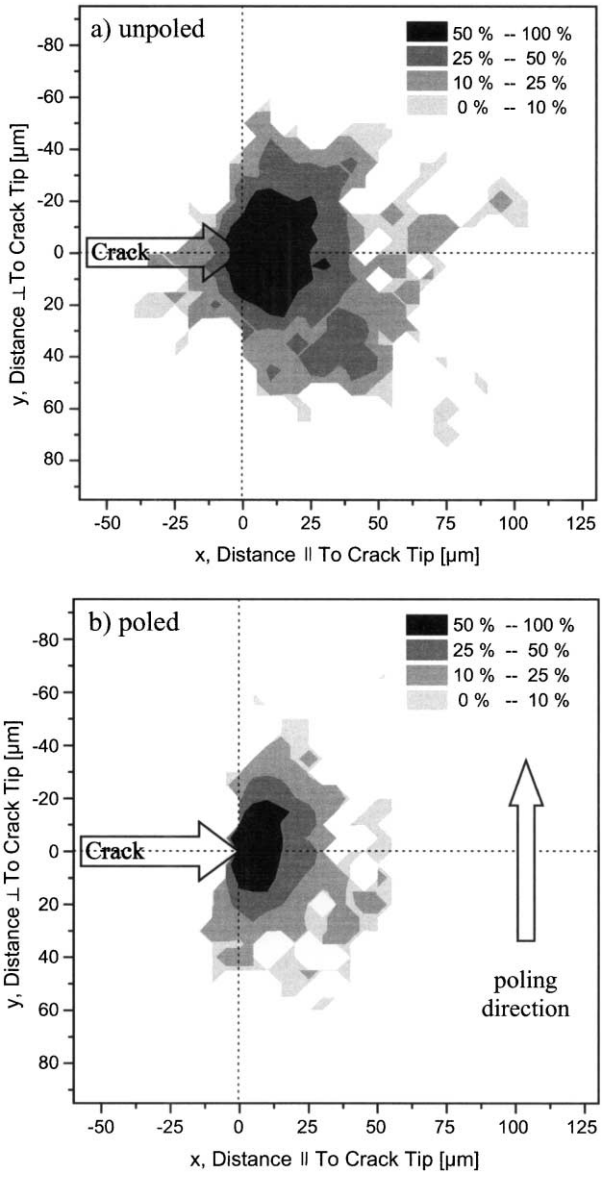

Fig. 9. Normalised distributions of switching events in (a) unpoled and (b) poled, coarse grained $BaTiO_3$. The crack tip is at (0,0), the crack heads towards positive x-values.

5. Conclusions

From this work, the following conclusions can be drawn:

- the toughness of coarse grained, unpoled $BaTiO_3$ with an average grain size of 20 μm decreases, if an electric field perpendicular to the crack is applied;

- if coarse grained $BaTiO_3$ with poling direction perpendicular to the crack is subjected to negative electric fields, the toughness is found to rise;
- the process zone in front of the crack tip can be measured in situ by investigation of crack growth using the Nomarski interference effect;
- the process zone in coarse grained $BaTiO_3$ is found to be larger for the unpoled state than for samples poled perpendicular to the crack. In addition, the amount of switching events is significantly smaller for the poled material;
- the toughness of fine grained $BaTiO_3$ with 0.4 μm average grain size is independent of crack length and electric fields up to 1 kV/mm.

Acknowledgements

The authors would like to thank Mr. Reinhard Mager for his help regarding sample preparation and crack growth measurements. This work was supported by the Deutsche Forschungsgemeinschaft.

References

1. Cook, R. F., Freiman, S. W. and Lawn, R. B., Fracture in ferroelectric ceramics. *Ferroelectrics*, 1983, **50**, 267–272.
2. Pohanka, R. C., Freiman, S. W. and Bender, B. A., Effect of the phase transformation on the fracture behavior of $BaTiO_3$. *J. Am. Ceram. Soc.*, 1978, **61**, 72–74.
3. Metha, K. and Virkar, A. V., Fracture mechanics in ferroelectric-ferroelastic lead zirconate titanate (Zr:Ti = 0.54:0.46) ceramics. *J. Am. Ceram. Soc.*, 1990, **73**, 567–574.
4. Zhang, Z. and Raj, R., Influence of the grain size on ferroelastic toughening and piezoelectric behavior of lead zirconate titanate. *J. Am. Ceram. Soc.*, 1995, **78**, 3363–3368.
5. Oh, K.-Y., Uchino, K. and Cross, L. E., Optical study of domains in $Ba(Ti,Sn)O_3$ ceramics. *J. Am. Ceram. Soc.*, 1994, **77**, 2809–2816.
6. Arlt, G., Twinnig in ferroelectric and ferroelastic ceramics: stress relief. *J. Mater. Sci.*, 1990, **25**, 2655–2666.
7. Eng, L. M., Güntherodt, H.-J., Schneider, G. A., Köpke, U. and Munoz Saldana, J., Nanoscale reconstruction of surface crystallography from three-dimensional polarization distribution in ferroelectric barium-titanate ceramics. *Applied Physics Letters*, 1999, **74**, 233–235.
8. Kolleck, A., Schneider, G. A. and Meschke, F. A., R-curve behavior of $BaTiO_3$- and PZT ceramics under the influence of an electric field applied parallel to the crack front. *Acta Mater.*, 2000, **48**, 4099–4113.
9. Meschke, F., Kolleck, A. and Schneider, G. A., R-curve behavior of $BaTiO_3$ due to stress-induced ferroelastic domain switching. *J. Eur. Ceram. Soc.*, 1997, **17**, 1143–1149.
10. Budiansky, B., Hutchinson, J. W. and Lambropoulos, J. C., Continuum theory of dilatant transformation toughening in ceramics. *Int. J. Solids Struct.*, 1983, **19**, 337–355.
11. Yamamoto, T., Igarashi, H. and Okazaki, K., Internal stress anisotropies induced by electric field in lanthanum modified $PbTiO_3$ ceramics. *Ferroelctrics*, 1990, **50**, 567–574.
12. Wang, H. and Singh, R. N., Crack propagation in piezoelectric ceramics: effects of applied electric fields. *J. Appl. Phys.*, 1997, **81**, 7471–7479.
13. Schneider, G. A. and Heyer, V., Influence of the electric field on Vickers indentation crack growth in $BaTiO_3$. *J. Eur. Ceram. Soc.*, 1999, **19**, 1299–1306.
14. Lynch, C. S., Fracture of ferroelectric and relaxor electric ceramics: influence of electric field. *Acta Mater.*, 1998, **46**, 599–608.
15. dos Santos e Lucato, S. L., Lupascu, D. C. and Rödel, J., Effect of poling direction on R-curve behavior in lead zirconate titanate. *J. Am. Ceram. Soc.*, 2000, **83**, 424–426.
16. Murakami, Y., *Stress Intensity Factors Handbook*. Pergamon Press, New York, 1987.
17. Kanninen, M. F., An augmented double cantilever beam model for studying crack propagation and arrest. *Int. J. Fract.*, 1973, **9**, 83–92.